Fourier Analysis of Single-Shot Dual-Energy X-ray Imaging Characteristics

Junwoo Kim[a], Dong Woon Kim[a], Ho Kyung Kim[a,b*]
[a]*School of Mechanical Engineering, Pusan National University, Busan, South Korea*
[b]*Center for Advanced Medical Engineering Research, Pusan National University, Busan, South Korea*
[*]*Corresponding author: hokyung@pusan.ac.kr*

1. Introduction

In previous studies [1, 2], single-shot dual-energy imaging (DEI) was developed using a flat-panel sandwich detector, and its capability was demonstrated by providing postmortem mouse DE images. The sandwich detector was realized by stacking two scintillator-based flat-panel detectors (FPDs) between which an intermediate copper (Cu) filter layer was placed to further enhance spectral energy separation. As a result, the proper selection of filter material and its thickness could be a trade-off between the extent of energy separation (hence, DE image quality) and image noise due to reduction in the number of x-ray quanta reaching the rear FPD. Although the conventional kVp-switching dual-shot method showed better image qualities than the single-shot method because of larger spectral energy separation, the motion-artifact-free DE image with reasonably good image quality was a potential prospect of the single-shot method.

For the reliable and better use of the sandwich detector for specific imaging applications, the sandwich detector should be optimally designed with a proper selection of scintillator material and thickness in each detector layer (i.e. the front and rear detectors), and aforementioned intermediate filter material and thickness. Recently, the performance-evaluation study of each detector layer consisting of the sandwich detector has been reported using the Fourier metrics such as the modulation-transfer function (MTF) and the Wiener noise-power spectrum (NPS), and the detective quantum efficiency (DQE) [3]. Although the concept of DE MTF, NPS, and DQE describing the performance of sandwich detectors was introduced by Richard and Siewerdsen [4], however, the performance of the sandwich detector itself has not been reported in experimental.

In this study, we quantitatively evaluate the imaging characteristics, such as MTF, NPS, and DQE in dual-energy images obtained from single-shot sandwich detector. Furthermore their properties for various imaging conditions, detector configurations, and operation parameters are investigated.

2. Materials and Methods

2.1 Single-Shot Detector System

As shown in figure 1, the sandwich detector may include the weighted logarithmic subtraction operation because one obtains only DE images as a result for the incidence of $\bar{q}_0$ to the detector, like tomographic images from a CT scanner.

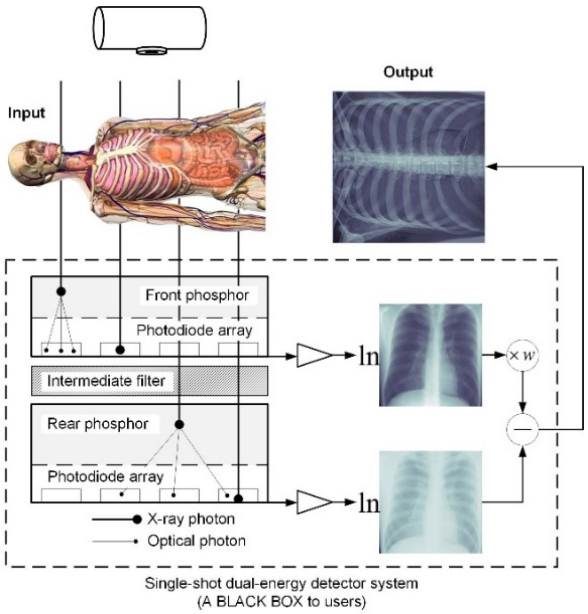

Fig. 1. Schematic illustration of a sandwich dual-energy detector. It may be considered as a single stand-alone detector.

The sandwich detector consisted of two FPDs which used the same photodiode arrays (RadEye1^{TM}, Teledyne Rad-icon Imaging Corp., Sunnyvale, CA) and gadolinium oxysulfide (Gd_2O_2S:Tb) phosphor screens (Carestream Health Inc., Rochester, NY) with different thickness: thinner (~ 34 mg cm^{-2}) for the front and thicker (~ 67 mg cm^{-2}) for the rear FPD layers, respectively. The photodiode array had 0.048 mm-sized pixels arranged 1024 × 512 format. Between the two FPDs, thin Cu sheet with a thickness t_{Cu} ranging 0.1 – 0.5 mm was inserted. Detailed designs and specifications of the sandwich detector can be found in references.

2.2 Measurement and Analysis

The sandwich detector was placed at a distance of 1 m from the focal spot of the x-ray tube (E7239X, Toshiba, Japan). The tungsten-anode x-ray tube had 2.4 mm aluminum-equivalent filtration and the tube voltage was varied between 50 and 90 kVp. The exposure time was fixed to be 0.2 seconds while the each detector read out images in 3 seconds. Entrance exposure at the front detector, X_F (mR), was measured with a calibrated ion chamber (Piranha R&F/M 605, RTI Electronics AB,

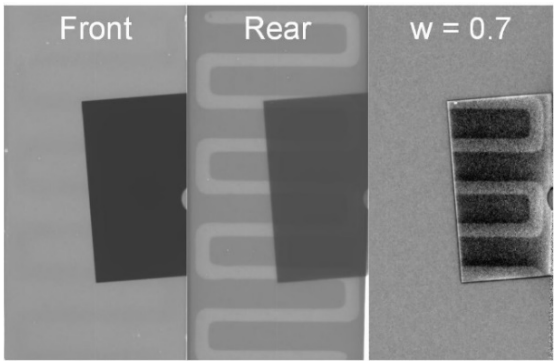

Fig. 2. Edge-phantom images obtained from the front and rear FPD layers, and their subtraction. The images were obtained at 60 kVp and t_{Cu} = 0.3 mm, and the dual-energy image was reconstructed with w = 0.7.

Sweden) and X_R at the rear detector after attenuation by the front detector and intermediate filter. The incident x-ray photon fluence was estimated using the calculated photon fluence per unit exposure and the measured exposures [5].

The MTF was evaluated from the images obtained for an edge-knife phantom. The edge profiles were extracted from the edge images, and the edge-spread functions (ESFs) were determined by least-squares regression analysis using

$$\begin{aligned}\mathrm{ESF}_{fit}(u) = \varsigma_1 + \xi_4\big[&\omega_1\big(1-e^{-\xi_1(x-x_0)}\big)\\ &+\omega_2 erf\{\xi_2(x-x_0)\}\\ &+\omega_3\big(1-e^{-\xi_3(x-x_0)^2}\big)\big]. \qquad (1)\end{aligned}$$

This fitting function is a modified version of that suggested by Boone and Seibert [6]. While the error function (erf) corresponds to the main lobe of the Gaussian shape in a line-spread function (LSF), the two exponential terms designate either side of LSF tails. The fitting parameters ω_j describe weights of each component of ESF and the parameters ξ_k describe extents. ς_1 describes the offset remained after bias correction on ESF. The original fitting function was composed of a single exponential term and the erf term with which computer fitting was separately performed for two regions: $x \geq x_0$ and $x < x_0$. However, this approach may result in a discontinuity around the inflection point. Fitting using Eq. (1) can avoid the discontinuity.

Weighted logarithmic subtraction was then performed for the fitted ESFs obtained from the front and rear FPDs. The subtracted ESF was subsequently differentiated to give rise to the corresponding LSF. By performing fast Fourier transformations (FFTs) to the LSF, we obtained the MTF result.

3. Preliminary Results

Figure 2 shows the edge-phantom images obtained from the front and rear FPD layers, and their subtraction. Unlike the images obtained from each FPD layer, the single-shot DE image showed dark-and-bright patterns around the edge phantom, which implied the large signal change around edges. It is noted that glue is used to adhere the fragile photodiode array onto the ceramic substrate and these glue patterns are apparent in the rear and DE images. The glue pattern in the rear image comes from the front FPD.

Unlike the conventional ESF as shown in Fig. 3(a), the ESF obtained from the subtracted image showed an enhancement as shown in Fig. 3(b). Consequently, the MTF obtained from the subtraction ESF showed a band-pass filter characteristic, as shown in Fig. 3(c), unlike the conventional low-pass filter characteristic (i.e., monotonic decrease of MTF value with increasing the spatial frequency). This MTF characteristic is due to the subtraction of two images with different spatial resolving powers (i.e., different thicknesses of phosphors between the front and rear detectors) as can be seen in unsharp masking digital image processing, which subtracts Gaussian-blurred image from the original image. This MTF characteristic implies that the sandwich detector loses the contrast performance at low spatial-spectral information content but relatively enhances that at mid spatial-spectral information content.

4. Ongoing and Further Studies

Further analysis of DE MTF is under progress. In addition, we are going to measure DE NPS and DQE. The results will be presented in detail. This study will be very useful for designing and optimizing sandwich detectors for single-shot dual-energy x-ray imaging.

ACKNOWLEDGEMENT

This work was supported by the National Research Foundation of Korea (NRF) grants funded by the Korea governments (MSIP) (No. 2013M2A2A9046313 and No. 2014R1A2A2A01004416).

REFERENCES

[1] S. Yun, J. C. Han, D. W. Kim, H. Youn. H. K. Kim, J. Tanguay, and I. A. Cunningham, Feasibility of active sandwich detectors for single-shot dual-energy imaging, *Proc. SPIE* 9033, pp. 90335T-90335T-8, 2014.
[2] J. C. Han, H. K. Kim, D. W. Kim, S. Yun, H. Youn. S. Kam, J. Tanduay, and I. A. Cunningham, Single-shot dual-energy x-ray imaging with a flat-panel sandwich detector for preclinical imaging, *Cur. Appl. Phys.*, Vol. 14, No. 12, pp. 1734-1743, 2014.
[3] J. Kim, D. W. Kim, S. Kam, H. Youn, and H. K. Kim, Effects of the energy-separation filter on the performance of each detector layer in the sandwich detector for single-shot dual-energy imaging, *accepted to J. Instrum.*, 2015.
[4] S. Richard and J. H. Siewerdsen, Optimization of dual-energy imaging systems using generalized NEQ and inaging task, *Med. Phs.*, Vol. 34, No. 1, pp. 127-139, 2007.
[5] H. Youn, J. Han, S. Yun, S. Kam, S. Cho, and H. K. Kim, Characterization of on-site digital mammography systems: Direct versus indirect conversion detector, *J. Korean Phys. Soc.*, Vol. 66, No. 12, pp. 1926-1935, 2015.

[6] J. M. Boone and J. A. SeibertAn analytical edge spread function model for computer fitting and subsequent calculation of the LSF and MTF, *Med. Phys.*, Vol. 21, No. 10, pp. 1541-1545, 1994.